J. Fluid Mech. (1982), *vol.* 121, *pp.* 301–313
Printed in Great Britain

Transitions in time-dependent thermal convection in fluid-saturated porous media

By G. SCHUBERT AND J. M. STRAUS

Space Sciences Laboratory, The Aerospace Corporation, P.O. Box 92957, Los Angeles, CA 90009

(Received 18 September 1981)

Numerical simulations of single-cell, two-dimensional, time-dependent thermal convection in a square cross-section of fluid-saturated porous material heated uniformly from below reveal a series of transitions between distinct oscillatory dynamical regimes. With increasing Rayleigh number R, the flow first evolves from steady-state behaviour into periodic motion with a single frequency f which depends on R approximately according to $f \propto R^{\frac{7}{8}}$; the transition Rayleigh number lies between about 380 and 400. At a value of R between about 480 and 500 the flow transforms into a fluctuating state characterized by two frequencies. Soon thereafter, for R between about 500 and 520, it reverts back to single-frequency periodic behaviour with f approximately proportional to $R^{\frac{3}{4}}$. The two frequencies in the narrow transition regime may be locked to a rational ratio, in which case the flow is periodic, or they may be commensurate, in which case the flow is quasi-periodic. The spectral characteristics of numerical realizations of unsteady convection and the occurrences of transitions therein are highly dependent on truncation level in Galerkin schemes or resolution in finite-difference approaches.

1. Introduction

Two-dimensional thermal convection in a fluid-saturated porous layer heated from below is known to become unsteady at sufficiently large Rayleigh number R (Combarnous & LeFur 1969; Caltagirone, Cloupeau & Combarnous 1971; Horne & O'Sullivan 1974; Caltagirone 1974, 1975). However, the Rayleigh number R_2 for the onset of this oscillatory behaviour has not been well determined. For single-cell convection in a square cross-section (the pattern of convection considered in this paper) Horne & O'Sullivan (1975) found $R_2 \simeq 280$. Caltagirone (1975), on the other hand, reported $R_2 = 384 \pm 5$, while Schubert & Straus (1979) determined R_2 to lie between 300 and 320. Some effort has been made to characterize the nature of the time-dependent flow for $R > R_2$. Based on finite-difference calculations with a 17×17 mesh at $R = 375$, 500, 750 and 1000, Horne & O'Sullivan (1974, 1978) concluded that this oscillatory flow is characterized by a single frequency f which is proportional to $R^{\frac{3}{4}}$.

Here we report the results of a detailed study of how single-cell, two-dimensional, time-dependent thermal convection in a square cross-section of fluid-saturated porous material heated uniformly from below depends on Rayleigh number. We show that the properties of this unsteady convection are very sensitive to truncation in a Galerkin computation (see also Marcus 1981), or equivalently to resolution in a finite-difference

calculation. Our previous determination of R_2 using the Galerkin technique was not carried out with a sufficient number of terms. The present calculations, which retain an adequate number of terms in the Galerkin expansion, place R_2 between 380 and 400, i.e. at $R = 380$ convection is steady while at $R = 400$ it is time-dependent. The character of oscillatory convection when $R > R_2$ is found to be more complicated than previously thought. In view of recent experience with the development of sequential instabilities in unsteady Taylor-vortex flow (e.g. Fenstermacher, Swinney & Gollub 1979) and time-dependent thermal convection (e.g. Gollub & Benson 1980), it is perhaps not surprising that we find transitions between distinct dynamical regimes in oscillatory porous-medium convection. For $R > R_2$ but less than a third transition Rayleigh number R_3, we observe a regular oscillatory flow with a single frequency f approximately proportional to $R^{\frac{7}{8}}$. Following Gollub & Benson (1980) we denote such a periodic oscillatory state as P. The transition Rayleigh number R_3 lies between about 480 and 500. For $R > R_3$ but less than a fourth transition Rayleigh number R_4, we find an unsteady regime with two basic frequencies. Gollub & Benson (1980) have labelled this a quasi-periodic QP_2 state if the frequencies are incommensurate or a periodic L-state if they are locked to a rational ratio. The transition Rayleigh number R_4 lies between about 500 and 520, so that the QP_2 (or L) regime occurs in a small range of R. Finally, for $R > R_4$ the flow returns to a periodic P-behaviour distinct from the P-regime at lower Rayleigh number. We have not carried out a sufficient number of calculations to determine the Rayleigh-number dependence of f unambiguously for these flows, but our results are consistent with $f \propto R^{\frac{1}{2}}$ for $R_4 \lesssim R \lesssim 650$. Thus the approximate Rayleigh-number interval 480 to 520 represents a multiple-frequency transition region between two periodic states. The evolution with Rayleigh number of single-cell, two-dimensional thermal convection in a square cross-section of fluid-saturated porous material heated from below is given by the sequence $S \rightarrow P \rightarrow QP_2$ (or L) $\rightarrow$ P, where S refers to steady state. Undoubtedly there are additional transitions. However, we have not observed any others for R between R_4 and 650.

We first provide a brief description of the mathematical model, the Galerkin technique, and the spectral analysis of the computed time-dependent flows. The results outlined above are then presented in detail.

2. Description of the mathematical model

Consider an infinitely long cylinder of fluid-saturated porous material with square cross-section. The bottom of the cylinder is at $z = 0$ and the top is at $z = d$; the vertical boundaries are at $x = 0, d$. The axis of the cylinder is parallel to the y-direction, and y extends from minus to plus infinity. The horizontal surfaces of the cylinder are isothermal, with T_0 the temperature at the top of the cylinder and $T_0 + \Delta T$ the temperature at the bottom ($\Delta T \geqslant 0$). The vertical walls are insulating. Both the horizontal and vertical surfaces of the cylinder are impermeable. Only time-dependent, two-dimensional, unicellular motions that are parallel to the (x, z)-plane will be treated. The governing equations and boundary conditions are (Straus 1974; Straus & Schubert 1979)

$$\nabla . \mathbf{u} = 0, \tag{2.1}$$

$$\nabla p + \alpha \rho \theta \mathbf{g} + \frac{\mu}{K} \mathbf{u} = 0, \tag{2.2}$$

$$\chi\frac{\partial\theta}{\partial t}+\rho c\mathbf{u}.\nabla\theta-\frac{w\Delta T}{d}=k\nabla^2\theta, \tag{2.3}$$

$$\theta=w=0 \quad (z=0,d), \tag{2.4}$$

$$\frac{\partial\theta}{\partial x}=u=0 \quad (x=0,d), \tag{2.5}$$

where $\mathbf{u}=(u,0,w)$ is the Darcy velocity of the volumetric flow rate of fluid per unit area of the porous medium, p is the pressure in excess of hydrostatic, ρ is the density, α is the coefficient of thermal expansion of the fluid, $\mathbf{g}$ is the acceleration due to gravity, μ is the fluid viscosity, K is the permeability, χ is the average heat capacity per unit volume of the fluid and solid matrix, c is the specific heat of the fluid, k is the average thermal conductivity of the fluid and matrix, and θ is the temperature in excess of the motionless conduction profile

$$\theta=T-T_0-\Delta T+\Delta T\frac{z}{d}. \tag{2.6}$$

These equations assume the validity of the Boussinesq approximation and Darcy's law.

We introduce dimensionless quantities according to

$$\xi=\frac{x}{d}, \quad \zeta=\frac{z}{d}, \quad \overline{\nabla}=d\nabla, \quad \tau=\frac{kt}{\chi d^2}, \tag{2.7}$$

$$\bar{\mathbf{u}}=(\bar{u},0,\bar{w})=\frac{\rho cd}{k}\mathbf{u}=\frac{\rho cd}{k}(u,0,w), \tag{2.8}$$

$$\overline{\theta}=\frac{\theta}{\Delta T}, \quad \overline{p}=\frac{K\rho c}{\mu k}p. \tag{2.9}$$

In terms of these dimensionless variables, the equations and boundary conditions become

$$\overline{\nabla}.\bar{\mathbf{u}}=0, \tag{2.10}$$

$$\overline{\nabla}\overline{p}+\bar{\mathbf{u}}-R\overline{\theta}\hat{\boldsymbol{\zeta}}=0, \tag{2.11}$$

$$\frac{\partial\overline{\theta}}{\partial\tau}+\bar{\mathbf{u}}.\overline{\nabla}\overline{\theta}=\overline{w}+\overline{\nabla}^2\overline{\theta}, \tag{2.12}$$

$$\overline{\theta}=\overline{w}=0 \quad (\zeta=0,1), \tag{2.13}$$

$$\frac{\partial\overline{\theta}}{\partial\xi}=\overline{u}=0 \quad (\xi=0,1), \tag{2.14}$$

where $\hat{\boldsymbol{\zeta}}$ is the unit vector in the ζ-direction, and the Rayleigh number is defined by

$$R=\alpha g\rho^2Kcd\Delta T/\mu k. \tag{2.15}$$

The two-dimensional continuity equation allows the introduction of a stream function in the form

$$\bar{u}=\phi_{\xi\zeta}, \quad \overline{w}=-\phi_{\xi\xi}, \tag{2.16}$$

where subscripts indicate differentiation. By substituting (2.16) into the curl of Darcy's law (2.11) one obtains

$$\theta=-\frac{1}{R}\overline{\nabla}^2\phi. \tag{2.17}$$

A single differential equation for ϕ together with appropriate boundary conditions follows upon substituting (2.16) and (2.17) into (2.12)–(2.14):

$$\frac{\partial}{\partial \tau}\bar{\nabla}^2\phi + \phi_{\xi\xi}\bar{\nabla}^2\phi_\xi - \phi_{\xi\xi}\bar{\nabla}^2\phi_\xi = \bar{\nabla}^4\phi + R\phi_{\xi\xi}, \tag{2.18}$$

$$\phi_{\xi\xi} = \phi_{\zeta\zeta} = 0 \quad (\zeta = 0, 1), \tag{2.19}$$

$$\phi_{\xi\zeta} = \bar{\nabla}^2\phi_\xi = 0 \quad (\xi = 0, 1). \tag{2.20}$$

As in our previous investigations (Straus 1974; Straus & Schubert 1979, 1981; Schubert & Straus 1979) we use the Galerkin technique to solve for ϕ. The Fourier-series expansion for ϕ,

$$\phi = \sum_{n=1}^{\infty}\sum_{j=0}^{\infty}\phi_{nj}(\tau)\sin n\pi\zeta\cos j\pi\xi, \tag{2.21}$$

identically satisfies the boundary conditions (2.19) and (2.20). The substitution of (2.21) into (2.18) yields an infinite set of coupled, nonlinear, first-order ordinary differential equations for $\phi_{nj}(\tau)$. These equations are truncated with $n+j \leqslant N$, where N is a positive integer, and solved numerically. The results reported here were obtained with $N = 14$, 16 and 18. We will see that the spectral properties of the oscillatory flows and the occurrences of transitions between different dynamical regimes depend strongly on the level of truncation. As a consequence one must be very careful to establish that any general conclusions are valid independent of N. For $N = 14$ there are 105 *a priori* non-zero coefficients ϕ_{nj}; for $N = 16$ the number of modes is 136 and for $N = 18$ it is 171. We employed the symmetry condition suggested by our previous calculations (Straus 1974; Schubert & Straus 1979), i.e. $n+j =$ a non-zero even integer, to reduce the number of non-zero coefficients to 56, 72 and 90, for $N = 14$, 16 and 18 respectively.

We will characterize the time dependence of the solutions by the variations which occur in the horizontally averaged upward heat flux q. The Nusselt number Nu is a dimensionless measure of q; it is given by

$$Nu = \frac{q}{k\Delta T/d} = 1 - \sum_{n=1}^{\infty}\frac{n^3\pi^3}{R}\phi_{n0}. \tag{2.22}$$

For a given R we calculate $Nu(\tau)$ and determine its spectral content by means of a fast-Fourier-transform algorithm. The Nusselt-number time series is computed for τ large enough to identify accurately the frequencies of any peaks in the power spectrum. The computations were carried out by starting at a value of R less than R_2 (the Rayleigh number for the S$\rightarrow$P transition) and determining $Nu(\tau)$ for successively larger R. The coefficients ϕ_{nj} at the end of a particular run were used to begin the calculation at the next higher value of R. The value of R_2 depends on truncation level; for $N = 10$, R_2 lies between 300 and 320 (Schubert & Straus 1979), for $N = 14$ it is between 370 and 380, and for $N = 18$ it is in the interval 380 to 400.

Table 1 is a summary of basic information about each $Nu(\tau)$ time series and the manner in which it was spectrally analysed. The total length of record refers to the total dimensionless time covered by the calculated $Nu(\tau)$ time series; this is usually much larger than the length of the record used in the spectral analysis. The part of the $Nu(\tau)$ data set that is spectrally analysed is always taken from the end of the time series in order to minimize the influence of any atypical initial transient behaviour. The Δf is a measure of the uncertainty in the frequency identification of spectral peaks.

R	Total length of record	Length of record in spectral analysis	Number of data points in spectral analysis	$\Delta\tau$	Δf
			$N = 14$		
380	0·993	0·310	6000	$5{\cdot}169 \times 10^{-5}$	3·2244
390	0·496	0·310	6000	$5{\cdot}169 \times 10^{-5}$	3·2244
400	0·496	0·496	9600	$5{\cdot}169 \times 10^{-5}$	2·0152
450	0·614	0·517	5000	$1{\cdot}0339 \times 10^{-4}$	1·9344
470	1·986	0·982	19000	$5{\cdot}169 \times 10^{-5}$	1·0182
480	1·985	0·992	19200	$5{\cdot}169 \times 10^{-5}$	1·0076
490	0·993	0·496	9600	$5{\cdot}169 \times 10^{-5}$	2·0152
500	3·475	0·982	19000	$5{\cdot}169 \times 10^{-5}$	1·0182
510	0·993	0·496	9600	$5{\cdot}169 \times 10^{-5}$	2·0152
520	0·993	0·496	9600	$5{\cdot}169 \times 10^{-5}$	2·0152
530	0·993	0·496	9600	$5{\cdot}169 \times 10^{-5}$	2·0152
550	0·993	0·496	9600	$5{\cdot}169 \times 10^{-5}$	2·0152
600	0·496	0·258	5000	$5{\cdot}169 \times 10^{-5}$	3·8692
620	0·496	0·258	5000	$5{\cdot}169 \times 10^{-5}$	3·8692
630	0·992	0·465	9000	$5{\cdot}169 \times 10^{-5}$	2·1496
650	1·488	0·465	9000	$5{\cdot}169 \times 10^{-5}$	2·1496
			$N = 16$		
450	0·495	0·257	6500	$3{\cdot}958 \times 10^{-5}$	3·887
480	1·484	0·257	6500	$3{\cdot}958 \times 10^{-5}$	3·887
500	1·089	0·257	6500	$3{\cdot}958 \times 10^{-5}$	3·887
520	0·990	0·257	6500	$3{\cdot}958 \times 10^{-5}$	3·887
550	3·463	0·257	6500	$3{\cdot}958 \times 10^{-5}$	3·887
600	0·495	0·257	6500	$3{\cdot}958 \times 10^{-5}$	3·887
650	0·495	0·257	6500	$3{\cdot}958 \times 10^{-5}$	3·887
			$N = 18$		
400	0·264	0·203	6500	$3{\cdot}127 \times 10^{-5}$	4·920
450	0·527	0·203	6500	$3{\cdot}127 \times 10^{-5}$	4·920
480	1·580	0·203	6500	$3{\cdot}127 \times 10^{-5}$	4·920
500	1·054	0·203	6500	$3{\cdot}127 \times 10^{-5}$	4·920
520	0·527	0·203	6500	$3{\cdot}127 \times 10^{-5}$	4·920
550	0·527	0·203	6500	$3{\cdot}127 \times 10^{-5}$	4·920
600	0·790	0·203	6500	$3{\cdot}127 \times 10^{-5}$	4·920

TABLE 1. Summary of basic information about each $Nu(\tau)$ time series and its spectral analysis.

3. Characteristics of time-dependent solutions

Transition 1: *onset of convection*

The critical Rayleigh number R_1 for the onset of convection in a square cross-section is $4\pi^2$ (Horton & Rogers 1945; Lapwood 1948). The ensuing two-dimensional motion is a steady S single-cell roll. In an infinitely long cylinder with a square cross-section, this flow is actually unstable to three-dimensional disturbances for $R \gtrsim 200$ (Straus 1974). Multicellular two-dimensional modes are also possible at sufficiently large Rayleigh number (Schubert & Straus 1979); for example, 2 rolls can occur within the square for $R \geqslant \frac{25}{4}\pi^2$. We will not be concerned with either three-dimensional or two-dimensional multicellular convection. Instead, we limit ourselves to unicellular two-dimensional motion and how it evolves through distinct time-dependent regimes with

increasing Rayleigh number. In the range of Rayleigh numbers considered here, multicellular two-dimensional convection is steady (Schubert & Straus 1979).

Transition 2: S→P

Unicellular convection in a square cross-section remains steady only for R smaller than a second transition Rayleigh number R_2. For $R > R_2$ single-cell convection is time-dependent. The value of R_2 is difficult to determine precisely because of the long integration times required to confirm the eventual decay of a very-small-amplitude motion. In addition, R_2 is dependent on the truncation number N. In an earlier study (Schubert & Straus 1979) we found steady convection at $R = 300$ and unsteady flow at $R = 320$ with $N = 10$. For $N = 12$ we also found steady convection at $R = 300$ and unsteady convection at $R = 400$. The present investigation makes clear that $N = 10$ and 12 are inadequate to determine R_2. With $N = 14$ we find that steady unicellular convection exists for R as large as 370; single-cell convection at $R = 380$ is time-dependent with extremely small amplitude at this level of truncation. For $N = 18$ we calculate a steady solution at $R = 380$ and an unsteady one at $R = 400$. Thus, our best estimate of R_2 is some value between 380 and 400.

Spectral analyses of $Nu(\tau)$ for flows with R slightly in excess of R_2 are characterized by peaks at a single fundamental frequency f and its harmonics. Following Gollub & Benson (1980) we denote such a periodic state as P. Transition 2 is of the type S→P. As the Rayleigh number is increased we find that unicellular convection remains periodic for $R < R_3$, a third transition Rayleigh number at which a bifurcation to a distinctly different time-dependent motion occurs. Figure 1 illustrates how the frequency of the fundamental spectral component increases with Rayleigh number for these periodic flows. A functional relationship of the form $f \propto R^{\frac{1}{2}}$ is a good fit to all the frequencies in the interval $R_2 < R < R_3$ independent of truncation number for $N = 14$, 16 and 18. The variance of the solutions undergoes a large increase with R near the onset of time-dependent convection, but it remains substantially constant throughout most of the interval R_2 to R_3 (figure 2). The higher harmonics of the fundamental frequency contribute relatively little to the total variance. The time-averaged Nusselt number $\overline{Nu}$ increases smoothly with R throughout this Rayleigh-number interval (figure 3). An example of a periodic state is shown by the regular oscillations of $Nu(\tau) - \overline{Nu}$ versus τ for $R = 480$ and $N = 18$ in figure 4. The figure also shows the power spectrum of this time series; the peaks at the fundamental frequency and its first three harmonics are clear.

Transition 3: P→QP_2 (*or* L)

The third transition in unicellular convection at $R = R_3$ marks a change from periodic motion with a single frequency to either quasi-periodic or periodic flow with two basic frequencies. An example of this more complicated time dependence is given by the $Nu(\tau) - \overline{Nu}$ time series at $R = 500$ and $N = 18$ shown in figure 5. Clearly, more than one frequency is involved. The power spectrum, also shown in the figure, reveals that there are two fundamental frequencies f_1 and f_2. Spectral peaks occur at frequencies that are sums, differences and harmonics of f_1 and f_2. In the classification scheme of Gollub & Benson (1980), a quasi-periodic oscillatory state with two fundamental incommensurate frequencies is denoted as QP_2. If the two frequencies are in a rational ratio then the state is actually periodic, and is labelled L. The solution in figure 5 is either QP_2 or

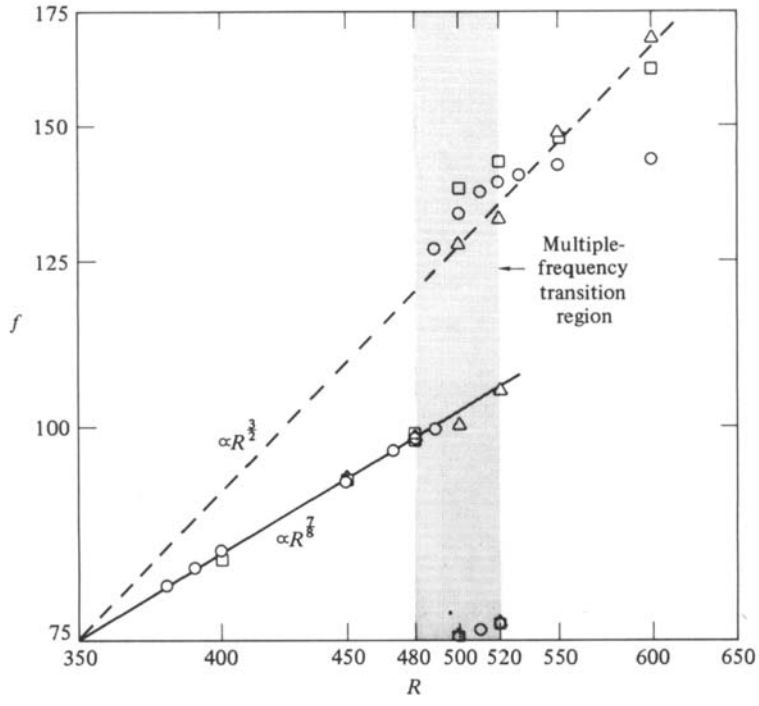

FIGURE 1. Dimensionless frequencies of peaks in the power spectra of $Nu(\tau)$. ○, $N = 14$; △, $N = 16$; □, $N = 18$. A narrow multiple-frequency transition region centred at $R = 500$ separates periodic regimes at lower and higher Rayleigh numbers. In the low-Rayleigh-number P-regime $f \propto R^{\frac{7}{8}}$; in the high-Rayleigh-number P-regime f is consistent with $f \propto R^{\frac{3}{2}}$.

L; although f_1/f_2 is approximately $\frac{7}{3}$, the frequency resolution of our power spectrum (see table 1) does not permit an unambiguous association of f_1/f_2 with the ratio of the two integers.

Quasi-periodic convection similar to that in figure 5 occurs over the Rayleigh-number range R_3 to R_4, where the latter Rayleigh number marks still another transition. All of the solutions in this Rayleigh-number interval have complex spectra with peaks at many frequencies. In all cases, the frequencies of the spectral peaks can be obtained from sums, differences and harmonics of two fundamental frequencies. Independent of truncation number these solutions all appear to be characteristically QP_2 or, within the limitations of our spectral resolution, L. Transition 3 is of the type $P \rightarrow QP_2$ (or L). We refer to the Rayleigh-number interval containing these solutions as a multiple-frequency transition region. This is because single-cell convection is periodic with a single frequency for $R > R_4$, making the interval R_3 to R_4 a transition between distinct P-regimes.

The values of R_3 and R_4 depend strongly on truncation number, but as shown by the shaded area in figure 1, the multiple-frequency transition region occurs between about $R = 480$ and $R = 520$. When $N = 14$, convection at $R = 470$ is of type P; it is QP_2 (or L) at $R = 480$, 490, 500, 510 and 520, and P at $R = 530$. At $N = 16$, the solutions at $R = 500$ and 520 are QP_2 (or L) and those at $R = 480$ and 550 are P. For $N = 18$, the states at $R = 480$ and 520 are P, while the one at $R = 500$ is QP_2 (or L). Thus the QP_2 (or L) states occur in a narrow Rayleigh-number interval centred at

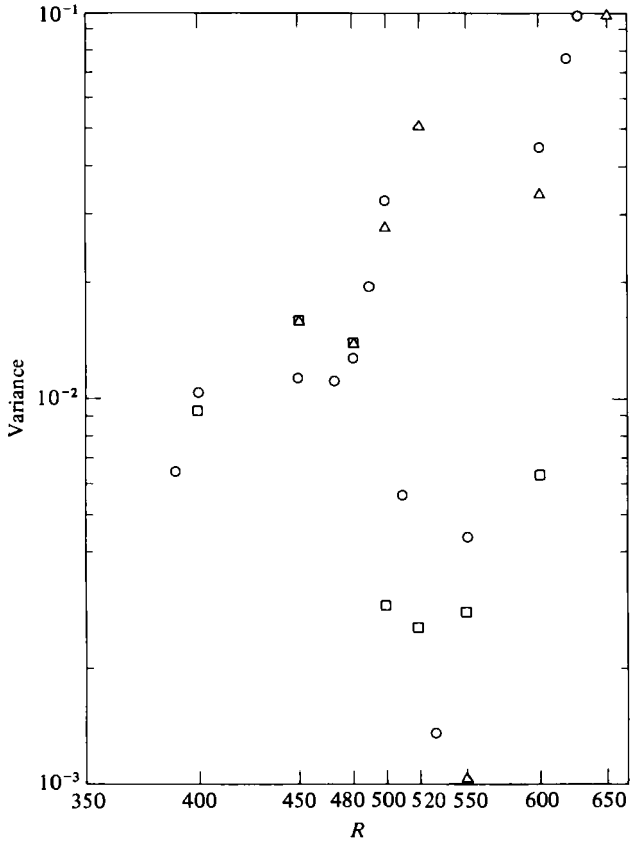

FIGURE 2. Variance of $Nu(\tau)$ time series as a function of Rayleigh number. Symbols have the same meaning as in figure 1.

$R = 500$. Based on these results we place R_3 between about 480 and 500, and R_4 between about 500 and 520.

Some of the characteristic frequencies associated with the QP_2 (or L) solutions are plotted in figure 1. The figure does not, however, record the frequencies of all the spectral peaks of these solutions. The mean Nusselt numbers $\overline{Nu}$ of the QP_2 (or L) states are given in figure 3, while the variances of the fluctuations in Nu are shown in figure 2. The transitions from P to QP_2 (or L) and QP_2 (or L) to P again are associated with a strong minimum in the variance of the Nu-oscillations. The location of the minimum along the R-axis, and the actual value of the minimum variance depend on truncation number N; however, a definite minimum is observed at all values of N. The minimum in the variance does not occur at a value of R within the multiple-frequency transition region. Even though the variance in Nu goes through a strong minimum, the time-averaged Nusselt number $\overline{Nu}$ increases steadily with R.

Transition 4: OP_2 (*or* L)$\rightarrow$P

As discussed just above, unicellular convection returns to a periodic state with one basic frequency if R is increased above R_4. An example of this is contained in figure 6 which shows $Nu(\tau) - \overline{Nu}$ versus τ and its power spectrum for $R = 520$ and $N = 18$. The

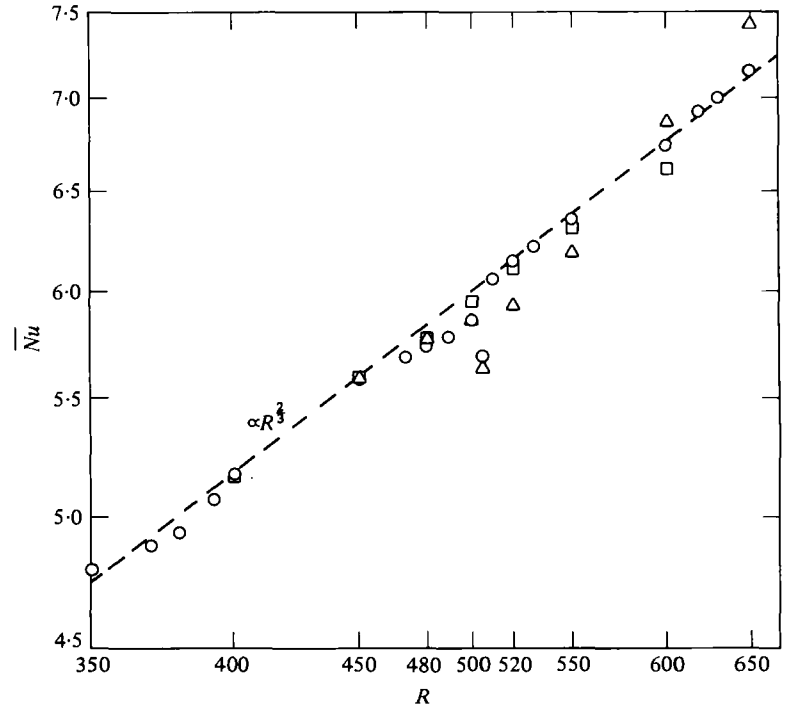

FIGURE 3. Time-averaged Nusselt number Nu as a function of R. Symbols are defined in figure 1. The dashed line represents $Nu \propto R^{\frac{2}{3}}$.

spectral peaks occur at a basic frequency and its first three harmonics. The fundamental frequencies in this second P-regime are shown as a function of Rayleigh number in figure 1 for R as large as 600 and $N = 14, 16, 18$. While these frequencies increase with R consistent with $f \propto R^{\frac{2}{3}}$, our computations do not extend over sufficiently large R to identify definitely the dependence of f on Rayleigh number in this regime. At a given R, the determinations of f for the different N show more scatter than they do in the periodic regime found at lower R. This probably indicates that N should be larger than 18 to determine $f(R)$ accurately in the second P-regime. Although our classification of the multiple-frequency transition region has not been precise (QP_2 or L), figure 1 leaves no doubt that there are two distinct P-regimes separated by a relatively narrow (in R) region of rapid adjustment. Figure 2 shows how the variance in the Nusselt-number fluctuations increases with R in the P-regime after attaining its transition-associated minimum value. Figure 3 shows the continued increase in $\overline{Nu}$ with R. The overall dependence of $\overline{Nu}$ on R is consistent with $\overline{Nu} \propto R^{\frac{2}{3}}$, but there are significant truncation-dependent departures of $\overline{Nu}$ from this relation.

4. Concluding remarks

The characteristics of time-dependent, single-cell, two dimensional convection in a square cross-section of porous material heated from below have been found to be strongly dependent on truncation number N. While modest levels of truncation may suffice to determine horizontally averaged properties of steady convection (e.g. Nu),

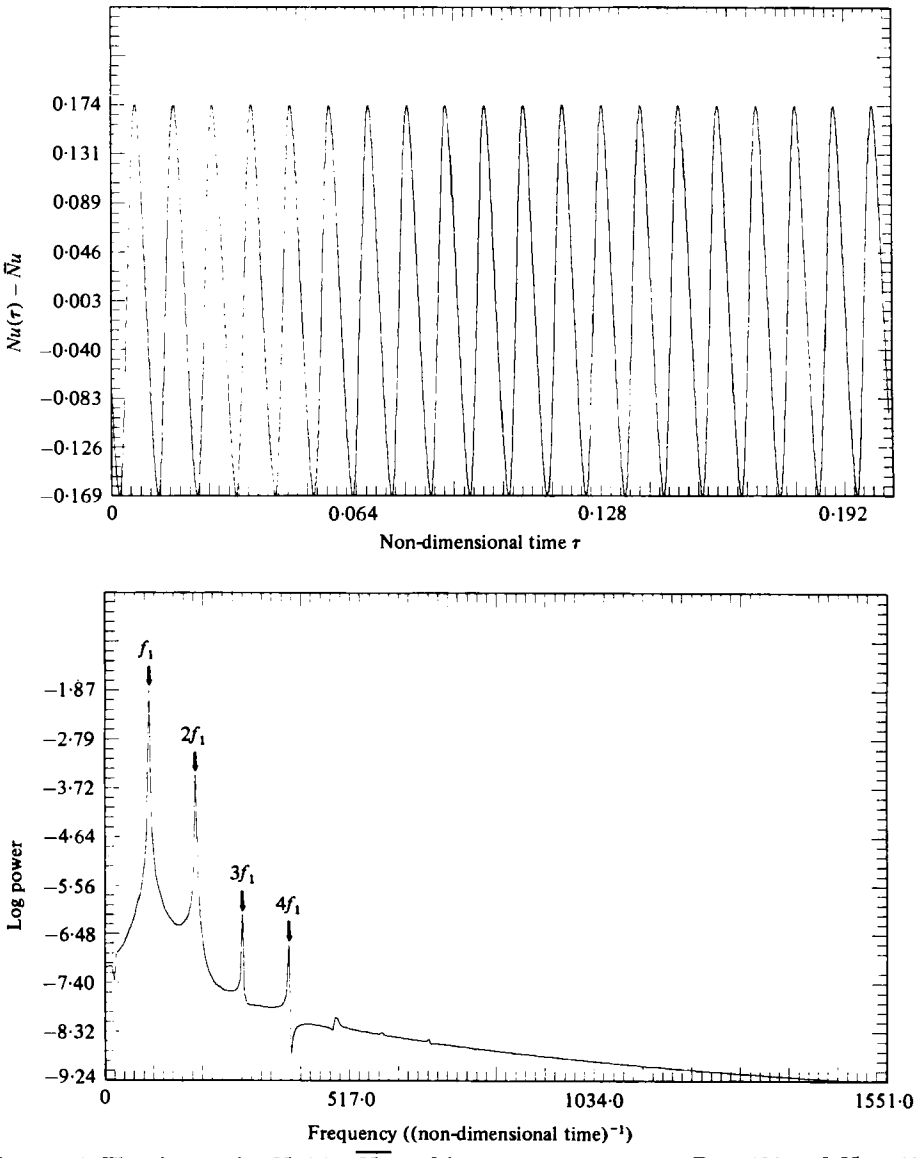

FIGURE 4. The time series $Nu(\tau) - \overline{Nu}$ and its power spectrum at $R = 480$ and $N = 18$. This is a periodic flow whose power spectrum is characterized by a single frequency f_1 and its harmonics $2f_1$, $3f_1$, and $4f_1$.

significantly more terms need to be retained in the Galerkin expansion (even at comparable Rayleigh numbers) to determine time-averaged and/or horizontally averaged properties (e.g. $Nu(\tau) - \overline{Nu}$) and spectral characteristics (e.g. peak frequencies) of unsteady convection. This implies that much finer grids are required to calculate time-dependent convective flows than steady flows when using finite-difference methods. Marcus (1981) was led to similar conclusions in his study of spherical convection using the Galerkin approach. If truncation is too severe it is possible to miss transitions. An extreme example of this is provided by the solutions of the single-mode

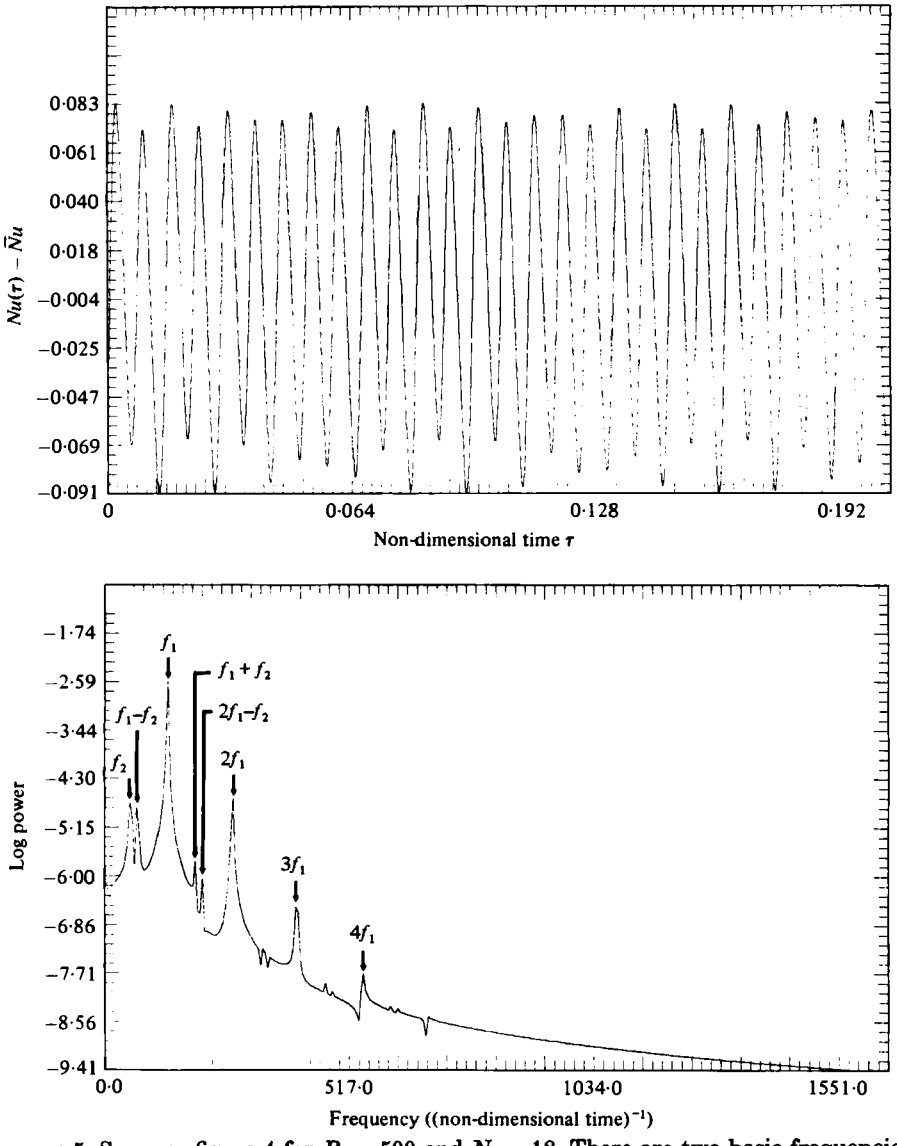

FIGURE 5. Same as figure 4 for $R = 500$ and $N = 18$. There are two basic frequencies f_1 and f_2 whose sums, differences and harmonics specify the frequencies of all spectral peaks. This is a quasi-periodic PQ_2 or periodic L flow.

equations of convection (Toomre, Gough & Spiegel 1977), which do not exhibit any of the known bifurcations to periodic or aperiodic states; these solutions are steady at all Rayleigh numbers. Over-truncation can also introduce transitions that do not really occur. At Rayleigh numbers slightly higher than those reported here, we have observed transitions with $N = 14$ that disappear when N is increased to 16 or 18 (for a discussion of similar effects in spherical convection see Marcus 1981). It is clear, when studying transitions in time-dependent flows, that the utmost care must be taken to avoid the introduction of spurious bifurcations as a consequence of insufficient horizontal resolution.

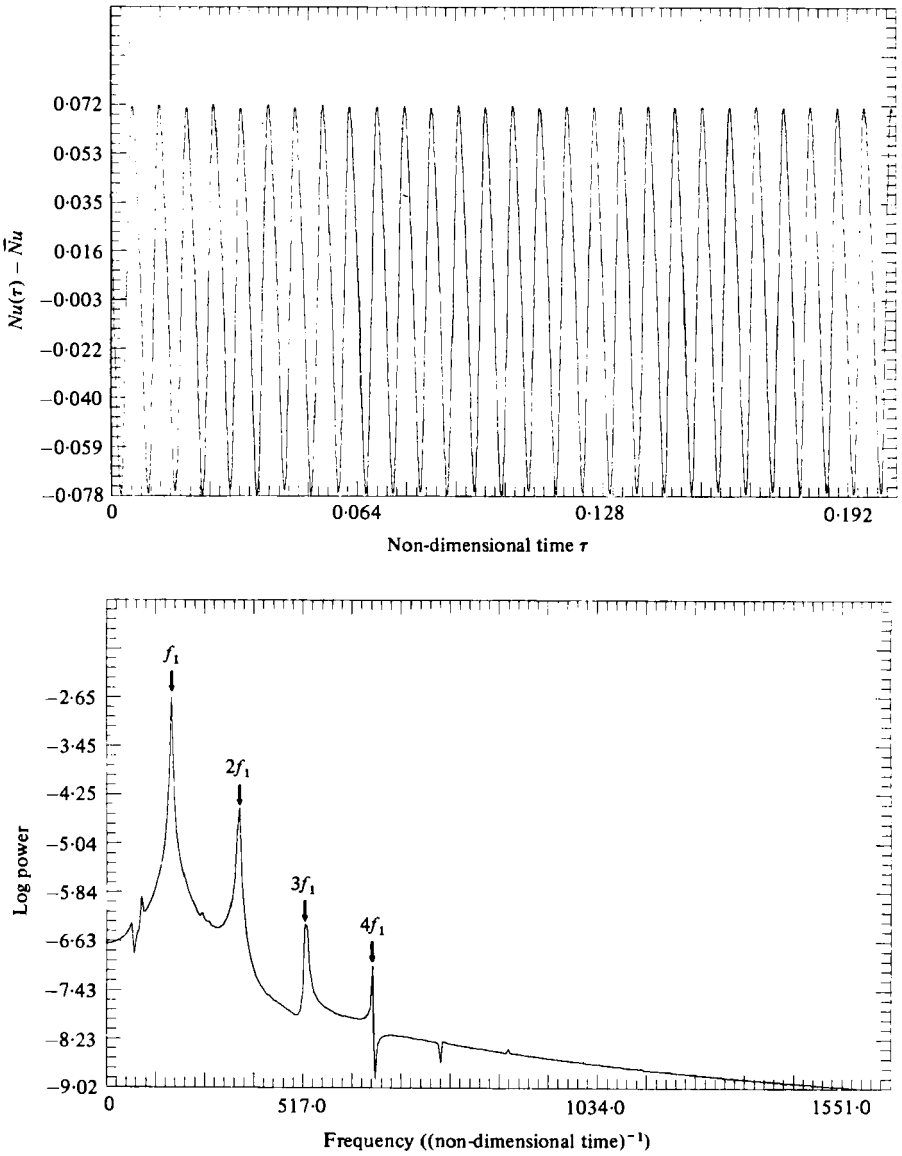

FIGURE 6. Same as figure 4 for $R = 520$ and $N = 18$. This is also a periodic flow with a single basic frequency and its harmonics.

The sequence of time-dependent instabilities that we observed may have been influenced by the symmetry condition we imposed (see the discussion after (2.21)). It has been found that the imposition of a similar symmetry requirement inhibits the transition to chaos in three-dimensional Rayleigh–Bénard convection (McLaughlin & Orszag 1982). Although our computations were not carried to sufficiently high Rayleigh number to attribute significance to the absence of an observed transition to chaos, the symmetry requirement may also modify the bifurcation sequence at Rayleigh numbers below that at which chaos occurs. Certainly, it would be worth while to repeat the study carried out here with the symmetry restriction removed.

This work was supported by the National Science Foundation under grant number ENG-76-82119.

REFERENCES

CALTAGIRONE, J. P. 1974 Convection naturelle fluctuante en milieu poreux. *C. R. Acad. Sci. Paris* **278** B, 259.

CALTAGIRONE, J. P. 1975 Thermoconvective instabilities in a horizontal porous layer. *J. Fluid Mech.* **72**, 169.

CALTAGIRONE, J. P., CLOUPEAU, M. & COMBARNOUS, M. 1971 Convection naturelle fluctuante dans une couche poreuse horizontale. *C. R. Acad. Sci. Paris* **273** B, 833.

COMBARNOUS, M. & LEFUR, B. 1969 Transfer de chaleur par convection naturelle dans une couche poreuse horizontale. *C. R. Acad. Sci. Paris* **269** B, 1009.

FENSTERMACHER, P. R., SWINNEY, H. L. & GOLLUB, J. P. 1979 Dynamical instabilities and the transition to chaotic Taylor vortex flow. *J. Fluid Mech.* **94**, 103.

GOLLUB, J. P. & BENSON, S. V. 1980 Many routes to turbulent convection. *J. Fluid Mech.* **100**, 449.

HORNE, R. N. & O'SULLIVAN, M. J. 1974 Oscillatory convection in a porous medium heated from below. *J. Fluid Mech.* **66**, 339.

HORNE, R. N. & O'SULLIVAN, M. J. 1978 Origin of oscillatory convection in a porous medium heated from below. *Phys. Fluids* **21**, 1260.

HORTON, C. W. & ROGERS, F. T. 1945 Convection currents in a porous medium. *J. Appl. Phys.* **16**, 367.

LAPWOOD, E. R. 1948 Convection of a fluid in a porous medium. *Proc. Camb. Phil. Soc.* **44**, 508.

MARCUS, P. S. 1981 Effects of truncation in modal representations of thermal convection. *J. Fluid Mech.* **103**, 241.

MCLAUGHLIN, J. B. & ORSZAG, S. A. 1982 Transition from periodic to chaotic thermal convection. *J. Fluid Mech.* (in the press).

SCHUBERT, G. & STRAUS, J. M. 1979 Three-dimensional and multicellular steady and unsteady convection in fluid-saturated porous media at high Rayleigh numbers. *J. Fluid Mech.* **94**, 25.

STRAUS, J. M. 1974 Large amplitude convection in porous media. *J. Fluid Mech.* **64**, 51.

STRAUS, J. M. & SCHUBERT G. 1979 Three-dimensional convection in a cubic box of fluid-saturated porous material. *J. Fluid Mech.* **91**, 155.

STRAUS, J. M. & SCHUBERT, G. 1981 Modes of finite-amplitude three-dimensional convection in rectangular boxes of fluid-saturated porous material. *J. Fluid Mech.* **103**, 23.

TOOMRE, J., GOUGH, D. O. & SPIEGEL, E. A. 1977 Numerical solutions of single-mode convection equations. *J. Fluid Mech.* **79**, 1.